COBEM 2023 27TH INTERNATIONAL CONGRESS OF MECHANICAL ENGENEERING

ABCM Brazilian Society of Mechanical Sciences and Engineering
27th ABCM International Congress of Mechanical Engineering
December 04-08, 2023, Florianópolis-SC, Brazil

COB-2023-0723
OCEAN CURRENT ESTIMATION FOR A TURRET-MOORED FPSO USING NEURAL NETWORKS

Pedro Felipe Lavra Dias
Gustavo Alencar Bisinotto
Anna Helena Reali Costa
Eduardo Aoun Tannuri
Universidade de São Paulo
{pedro.lavradias; gustavo.bisinotto; anna.reali; eduat}@usp.br

Abstract. *This research deals with a data-driven model to estimate local ocean currents affecting a Turret-Moored FPSO. Strong environmental conditions impact the effectiveness of oil exploration at deep sea, reducing the uptime and increasing risks. With Turret–moored FPSOs, due to their hull-shaped format and the weathervaning property, crucial importance is given to onboard sensors capable of estimating these conditions and platform response. The accurate measurement of ocean currents is difficult with ordinary onboard devices. Hence, a motion-based Multi-Layer Perceptron Neural Network (MLP) is proposed to determine local current speed and direction. A dataset of environmental conditions observed in a Brazilian offshore oil basin was input to numerical simulations with two loading conditions: full-loaded and ballasted. Those simulations provided time-domain platform responses from which motion statistics were computed to generate a dataset that was associated with wind speed and direction to train four Neural Networks: two for each loading condition – one for current speed and the other for current direction. Results demonstrated a strong relationship between estimations and references (correlations around 70% and 90% for current speed and direction, respectively) and mean absolute errors of 0.09 m/s and 25° for full-load, and 0.09 m/s and 30° in ballast.*
Keywords: *Turret-Moored FPSO, Neural Networks, Estimation of Ocean Current.*

1. INTRODUCTION

Floating, Production, Storage, and Offloading Platforms (FPSO) are being increasingly used to explore oil and natural gas in deep-sea around the globe. Especially in Brazil, where more than 95% of the biofuels are located at sea, these hull-shaped platforms have acquired significant relevancy in recent years (Brasil, 2020).

Due to the variability of the environmental conditions on the Southeast Offshore Brazilian Basins, FPSO platforms might be moored by a pivoting mechanism - called Turret (Figure 1a) - which is often placed near the platform bow. This equipment allows the FPSOs to weathervane (Figures 1b and 1c) on the prevailing environmental conditions (Nair *et al.*, 2019). It also enables the use of fewer and less-stressed mooring lines, besides the improvement of offloading process to Shutter Tankers (Howell *et al.*, 2006; England *et al.*, 2001).

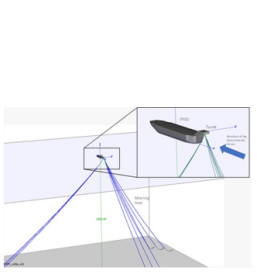

(a) Computer model of a Turret-FPSO

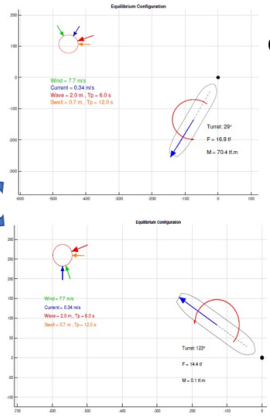

(b) Weathervanning property:
- ***Heading:*** *029°*
- ***Wind*** *(green arrow)**:** Speed: 7.7 m/s; Direction: 330°*
- ***Current*** *(blue arrow)**:** Speed: 0.34 m/s; Direction: 190°*
- ***Wave*** *(red arrow)**:** Height: 2 m; Period: 6s; Direction: 085°*
- ***Swell*** *(orange arrow)**:** Height: 0.7m; Period: 12s; Direction: 090°*

(c) Weathervanning property:
- ***Heading:*** *123°*
- ***Wind*** *(green arrow)**:** Speed: 7.7 m/s; Direction: 175°*
- ***Current*** *(blue arrow)**:** Speed: 0.34 m/s; Direction: 000°*
- ***Wave*** *(red arrow)**:** Height: 2 m; Period: 6s; Direction: 085°*
- ***Swell*** *(orange arrow)**:** Height: 0.7m; Period: 12s; Direction: 090°*

Figure 1: Model of Turret-FPSO and weathervanning characteristic

Analyzing Figure 1, one can observe the strong relationship between platform motions and environmental conditions. Due to this fact, the present study treats the inverse problem, that is: estimating local ocean currents (speed and direction) by applying data-driven strategies based on the platform motions: Heading, Standard Deviations of heave, roll, pitch, and

yaw plus the wind speed and direction. Movements with vertical components are considered proxy/indirect measurements of wave forces.

The process of estimating environmental conditions with data-driven methods is increasing in modern research. Most studies have considered data from meteorological/oceanographic sensors, such as buoys, radars, and satellites, to derive models for estimating metocean variables.

Examples of such studies may be found in Faniband and Shaahid (2020), which have implemented a Multi-Layer Perceptron (MLP) to forecast wind speed in Saudi Arabia, taking as input past values of measured wind speed, humidity, temperature, and elevation. Also in the research of Podrazka *et al.* (2022), who trained Long-Short Term Memory and Densely Connected Neural Networks for sea state estimation based on buoys measurements data from the Gulf of Mexico; and Thongniran *et al.* (2019), which improved the estimation accuracy of ocean currents data - collected from high-frequency radar stations - in the Gulf of Thailand by adding domain knowledge to the Convolutional Neural Networks (CNN) and the Gated Recurrent Unit (GRU).

More recently, researchers have used ship motions, instead of measuring devices, to estimate environmental conditions in specific regions. For example, Han *et al.* (2021) proposed an ensemble of Machine Learning algorithms to make a real-time estimation of sea state characteristics based on ship motions. Similarly, Bisinotto *et al.* (2023) studied a Spread Moored FPSO placed at a Brazilian Offshore Basin and used Convolutional Neural Networks to estimate wave height, peak period, and mean direction.

In a previous study of this research project, Dias *et al.* (2022) proposed an estimation model for ocean currents based on the motions of a fully loaded Turret-FPSO. The authors first applied K-Means algorithms to classify platform motions and then implemented Neural Networks models to estimate ocean currents. This paper expands the previous study with the application of an MLP Neural Network to estimate local ocean currents acting on a Turret-Moored FPSO for two loadings conditions: full load and ballast, drafts of 15.6m and 10.5 m, respectively. The features used are only the commonly on-board collected measurements: wind speed and direction (measured via anemometer and anemoscope); platform Heading (obtained by GPS or Magnetic/Gyro compass); and FPSO oscillating motions that are given by the standard deviation of heave, roll, pitch and yaw (measured by MRU sensors).

The text is structured as follows. Section 2 covers the methods applied to make the estimations. Section 3 presents the results of the proposed solution, discussing the effects of the unbalanced dataset on MLP models and Section 4 brings the conclusion.

2. MATERIALS AND METHODS

This section presents the research methodology, which was divided into three phases (Figure 2): Dataset Generation, Regressor Algorithm and Post-Processing.

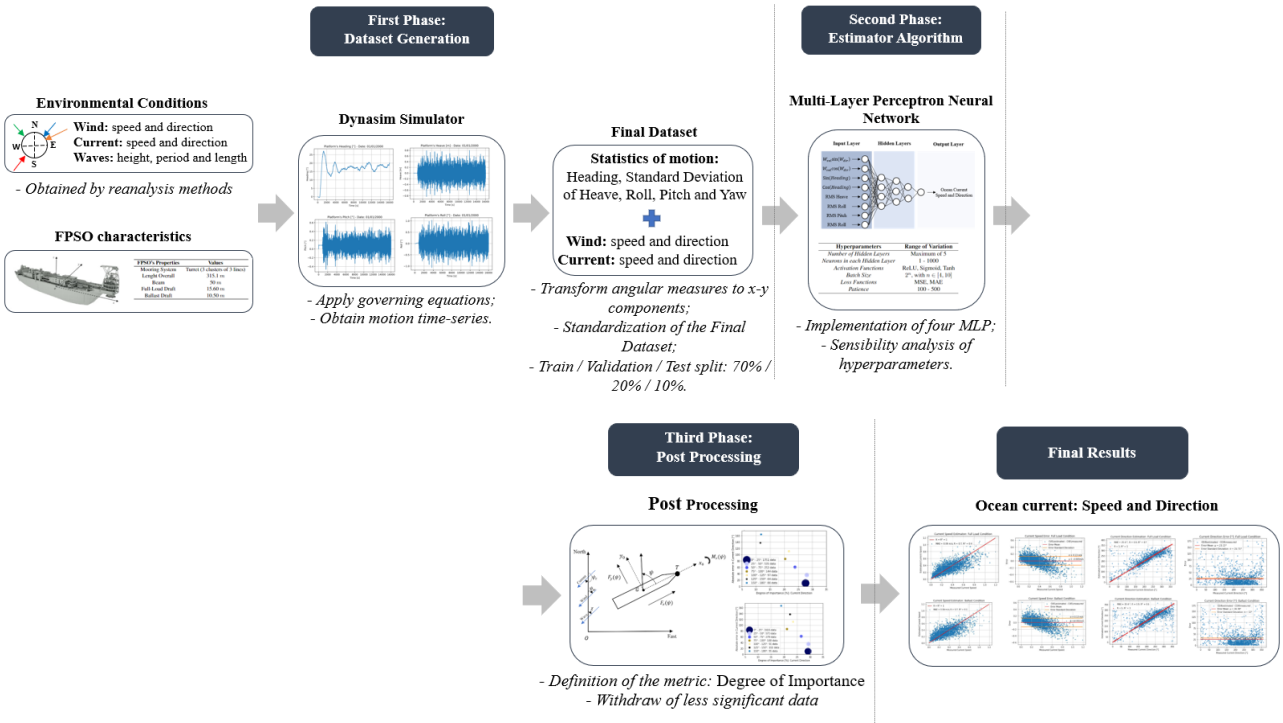

Figure 2: Research Pipeline.

The platform in the study is anchored in the proximity of Rio de Janeiro and São Paulo coast at a depth of approximately 2,000 meters. It has a mooring system of the Turret type, allowing the platform to weathervane to the environmental conditions. Table 1 gives some characteristics of the FPSO.

Table 1: FPSO's characteristics

FPSO's Properties	Values
Mooring System	Turret (3 clusters of 3 lines)
Lenght Overall	315.1 m
Beam	50 m
Full-Load Draft	15.60 m
Ballast Draft	10.50 m

The data used in the estimation process consisted of environmental conditions obtained from a Hindcast model considering the platform location (Lima *et al.*, 2013). These data were denominated as *Initial Dataset* and consisted of 29,225 environmental conditions.

These conditions represent the environmental characteristics over a period of 10 years (01/01/2000 to 01/01/2010), at a 3-hour time stamp, which are summarized in Table 2, where: W_{vel} and W_{dir} are the wind speed, at 10 m height, and the wind direction (from where it comes) in relation to true North; C_{vel} and C_{dir} are the surface current speed and direction (to where it goes); $W_{1height}$ and $W_{2height}$ are the significant wave heights associated to two wave components; $W_{1period}$ and $W_{2period}$ are the wave peak periods; W_{1dir} and W_{2dir} are the mean wave directions (from where it comes).

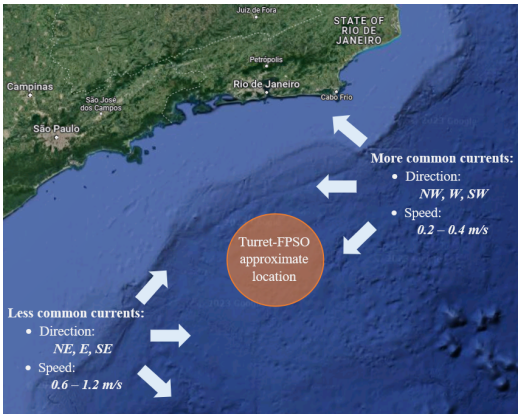

Figure 3: Map of Ocean Currents

To achieve a better understanding of the data input into the regressor algorithms and their performance limits, a brief analysis of the available metocean data is carried out. Due to the geographical position of Brazil, and the Oceanic Circulation Pattern (South Atlantic Gyre (Lobo, 2019)), most ocean currents on the Brazilian Coast have a Southwest direction (Figure 3). Hence, it is expected the dataset of environmental conditions to be unbalanced with respect to the ocean current direction, which influences the training of the data-driven algorithms, especially for ocean currents with less frequent occurrences.

Table 2: Initial Dataset.

Environmental Conditions	Mean	Standard Deviation	Minimum value	Maximum value
W_{vel} $[m/s]$	7.69	2.54	0.90	17.63
W_{dir} $[^o]$	68.13	36.25	0.00	360
C_{vel} $[m/s]$	0.34	0.19	0.00	1.31
C_{dir} $[^o]$	235.5	40.38	0.00	360
$W_{1height}$ $[m]$	1.97	0.63	0.78	7.85
$W_{1period}$ $[s]$	8.59	2.36	3.72	20.70
W_{1dir} $[^o]$	70.15	58.31	0.10	358.70
$W_{2height}$ $[m]$	0.66	0.59	0	3.15
$W_{2period}$ $[s]$	4.63	4.07	0	20.67
W_{2dir} $[^o]$	90.78	90.64	0	360

2.1 Dataset Generation

To assess the platform response, the *Initial Dataset* was input into a Time Domain Simulator for the Moored Platform – DYNASIM (Nishimoto *et al.*, 2002), developed by Petrobras and Brazilian Universities, including the University of São Paulo (USP). The outputs of the simulations are the time-domain (16,000 seconds) Platform responses for each environmental condition.

Statistics of motion - heading and the Standard Deviation of heave, roll, pitch, and yaw - were computed for the final 8,000 seconds of the simulations, corresponding to the steady-state platform response. These statistics (presented in Table 3) and the wind properties (from Table 2) consist of the MLP inputs, which are associated with the ocean current information (reference for the MLP outputs), also presented in Table 2, to generate the *Final Dataset*.

Table 3: Statistics of Motion.

	Full-Load		Ballast	
Statistic of Motion	**Mean Value**	**Standard Deviation**	**Mean Value**	**Standard Deviation**
$Mean\ Heading\ [^o]$	86.09	55.54	86.11	56.61
$RMS_{Heading}\ [^o]$	2.07	1.37	1.92	1.43
$RMS_{Heave}\ [m]$	0.12	0.13	0.11	0.12
$RMS_{Pitch}\ [^o]$	0.11	0.09	0.12	0.11
$RMS_{Roll}\ [^o]$	0.18	0.27	0.25	0.35

After defining the final dataset, these data were randomly divided, following a 70/20/10 split, into training, validation, and test sets. This process is important when dealing with data-driven algorithms since the training data are used to update the weights, the validation data to optimize the hyperparameters of the model, and the test data to verify the generalization of the system to previously unseen inputs. To improve the numerical convergence of the learning algorithm in training the neural network, a Z-score Standardization method was applied to all three datasets, using the statistical properties (mean value and standard deviation) of the training set.

2.2 Regressor Algorithm

The proposed regressor algorithm is an MLP Neural Network. This mathematical model essentially aims to estimate the mapping between a set of input variables to an output or a set of output values. The best function approximation is obtained by adjusting learnable parameters from the available data (Goodfellow and Courville, 2016).

One of the greatest benefits of MLP Neural Networks is the development of higher-order polynomial hypothesis functions, which can find hidden patterns among the input features. Each element of a neural network (commonly known as a neuron) applies an activation function $f(x)$, into a linear combination (weighted sum) of the outputs of the previous layers to generate its own output (Eq. 1):

$$\hat{y}_i = f\left(w_o + \sum_{i=1}^{n} w_i x_i\right), \tag{1}$$

where $\hat{y}_i$ is the output of each neuron and x_i are its inputs, w_i represent the learnable weight to be adjusted during the training process.

The inputs of the network are wind speed, wind direction, mean heading, standard deviation of heave, roll, pitch, and yaw. Angular measures are projected into their rectangular coordinates, as shown in Figure 4, which is a common approach when dealing with circular quantities.

The number of hidden layers and the number of neurons in each hidden layer is optimized in the sensitivity analysis. For the output layer, it is applied a linear function that correlates the estimations with the reference value of current speed/direction through a loss function.

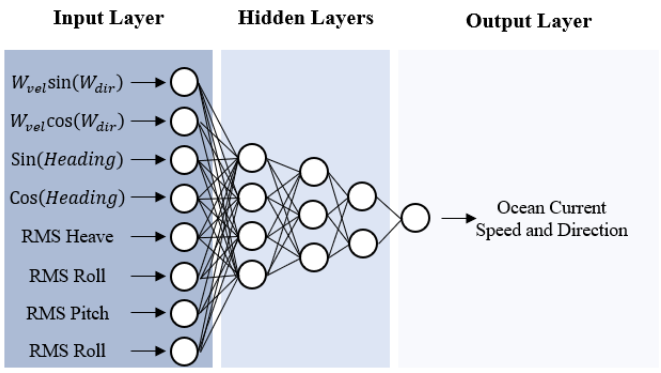

Figure 4: Illustrative representation of the Neural Networks

Two loss functions are considered to update the weights: the Mean Squared Error (Eqs. 2) and the Mean Absolute Error (Eqs. 3). Equations with subscript "*circular*" apply only to the current direction.

$$MSE = \frac{1}{N}\sum_{i=1}^{N}\left(y_i - \hat{y}_i\right)^2; \quad MSE_{circular} = \Omega\left[H\left(y_i - \hat{y}_i\right)\right]^2; \tag{2}$$

$$MAE = \frac{1}{N}\sum_{i=1}^{N}\left|y_i - \hat{y}_i\right|; \quad MAE_{circular} = \Omega\left[H\left(y_i - \hat{y}_i\right)\right], \tag{3}$$

where y_i is the reference current speed/direction (*target values*) and $\hat{y}_i$ are the estimated ones (Eq. 1), N represent the number of examples tested, $H(x) = \min\left(|x_i - x_j|, |x_j - x_i|\right)$ is the result of angular values subtraction and $\Omega(x) = \arctan\left[\frac{\frac{1}{N}\sum_{i=1}^{N}\sin x_i}{\sum_{i=1}^{N}\cos x_i}\right]$, is the circular mean.

These loss functions (Eqs. 2 - 3), along with the Pearson Correlation Coefficient (R) and the Coefficient of Determination (R^2), are the metrics used to evaluate the performance of the estimations.

One hindrance of Neural Networks is the large number of possibilities that can structure the algorithm. In the study made by Suller *et al.* (2021), the authors tested three different approaches to optimize the number of neurons in the hidden

layer: Bayesian Optimization, Random Search and Simulated Annealing. The results showed that the Random Search presented a similar performance to the best method found (Bayesian Optimization), but it is easier to implement and requires less computational effort.

Therefore, this research created 5,000 random configurations of hyperparameters and tested each design to estimate the four ocean current parameters considered in the study (current speed and direction for full-load and ballast). The search space of hyperparameters is summarized in Table 4.

Table 4: Tested Hyperparameters

Hyperparameters	**Range of Variation**
Number of Hidden Layers	Maximum of 5
Neurons in each Hidden Layer	1 - 1000
Activation Functions	ReLU, Sigmoid, Tanh
Batch Size	2^n, with $n \in [4, 10]$
Loss Functions	MSE, MAE
Patience	100 - 500

The maximum number of epochs was fixed as 1,000 and the Optimizer used was the Adaptive Moment Estimation (Adam). The term *Patience* refers to the *Early Stopping* technique to avoid *overfitting*. It controls the number of epochs with no changes in the validation metrics and stops training when the patience value is achieved. All the implementation in this research was done with Python libraries.

2.3 Post Processing

Platform response to external loads is nonlinear, and can exist more than one equilibrium position for the same environmental condition. Hence the inverse estimation of ocean currents from the platform response defines an ill-posed problem, which even powerful MLP algorithms are not able to cope with.

Besides that, there are cases where the ocean current effects on the FPSO equilibrium position are so small that, regardless of its direction, the platform response would be essentially the same.

It is also worth noticing the directional character of the environmental conditions (Figure 3). This creates challenges to the data-driven estimation, since an unbalanced dataset may influence the machine learning algorithm to be biased towards the most common data.

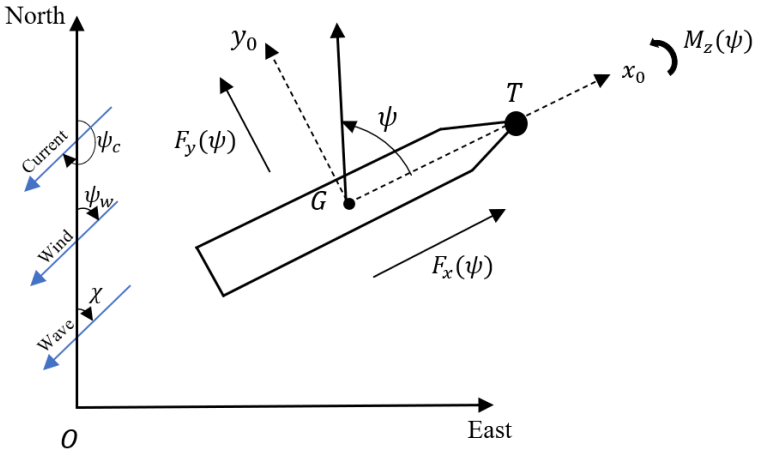

Figure 5: Coordinate axis and Resultant Forces

Due to these issues, it is proposed a post-processing strategy to treat the MLP estimations. This process consists of withdrawing ocean current estimations that do not effectively contribute to the equilibrium position of the platform.

Figure 5 illustrates the environmental forces (blue arrows) acting on a Turret-FPSO and the reaction forces ($F_x(\psi), F_y(\psi)$) and moment ($M_z(\psi)$) acting on point G (Center of Gravity). For clarity, "ψ" is the FPSO equilibrium heading, and "ψ_C", "ψ_W" and "χ" are the incidence angle of current, wind and waves, respectively.

Wind and ocean current forces acting on the platform center of gravity can be modeled by taking into account their relative velocity (V_{Wr} and V_{Cr}) and direction ($\psi_{Wr} = |180 + \psi - \psi_W|$ and $\psi_{Cr} = |\psi - \psi_C|$) with respect to the platform heading. Equation 4 presents a model for the ocean current loads on the platform with respect to the Gx_oy_o frame, solidary to the body.

$$F_x^{current} = \tfrac{1}{2}\rho_c L D C_{Cx}(\psi_{Cr}) V_{Cr}^2; \quad F_y^{current} = \tfrac{1}{2}\rho_c L D C_{Cy}(\psi_{Cr}) V_{Cr}^2;$$
$$M_{zz}^{current} = \tfrac{1}{2}\rho_c L^2 D C_{Cz}(\psi_{Cr}) V_{Cr}^2, \tag{4}$$

where $F_x^{current}, F_y^{current}$ and $M_{zz}^{current}$ are the ocean current forces and moment, ρ is the mass density of the salt water, $C_{Cx}(\psi_{Cr}), C_{Cy}(\psi_{Cr})$ and $C_{Cz}(\psi_{Cr})$ are the current coefficients (dependent on the type of the ship and relative direction), L is the platform length between perpendicular and D, platform draft. Physical models may be also obtained for the wind loads F_x^{wind}, F_y^{wind} and M_{zz}^{wind}, and wave effects F_x^{wave}, F_y^{wave} and M_{zz}^{wave}, as shown in Tannuri *et al.* (2014).

The *Final Dataset* consists of the equilibrium statistics of motion. From Newton's Second Law, the sum of all the forces and moments at any point of the platform in equilibrium is equal to zero. Thus, $F_x(\psi) = F_y(\psi) = M_z(\psi) = 0$, representing the net forces/moments from the contributions from wind, current, and wave forces/moments, and the mooring system.

Nonetheless, the mooring forces are not easily available, which makes the point "T" - platform Turret location (Figure 5) - an interesting candidate to evaluate the equilibrium of moments, as the lever arm of the mooring forces is zero. For this purpose, the moments generated by the environmental conditions are transferred from the center of gravity to point "T" with the following expressions:

$$M_T^{wind;current;wave} = -\tfrac{L}{2} F_y^{wind;current;wave} + M_{zz}^{wind;current;wave}, \tag{5}$$

where M_T^{wind}, $M_T^{current}$ and M_T^{wave} are the wind, current and wave moments with respect to Turret location, respectively.

After computing the moments in Eq. 5, the metric Degree of Importance (*DoI*) in the Equilibrium Heading can be deduced by:

$$DoI_{current} = \frac{|M_T^{current}|}{|M_T^{current}| + |M_T^{wind}| + |M_T^{wave}|} \, . \tag{6}$$

With this metric, all estimated currents with a Degree of Influence less than 30% were eliminated from the results.

3. RESULTS

3.1 Hyperparameter Optimization

Firstly it is presented the results of the optimization process to define the network architecture. Table 5 brings the best two configurations for each four Neural Networks implemented. The metrics are given with respect to the validation set.

Table 5: Sensitivity Analysis

Loading	**Target**	**MLP configuration**					**Metrics**		
		Neurons per Layer	*Act.*	*Batch*	*Loss*	*Pat.*	*MAE*	*R*	R^2
Full Load	*CVEL*	[8-785-928-281-1]	ReLU	128	MSE	136	0.09 m/s	75%	60%
		[8-703-646-266-1]	ReLU	128	MSE	361	0.09 m/s	75%	55%
	CDIR	[8-746-201-332-157-668-1]	ReLU	512	MAE	342	33.45^o	85%	60%
		[8-868-713-796-812-787-1]	ReLU	32	MAE	423	33.58^o	83%	58%
Ballast	*CVEL*	[8-346-895-950-963-275-1]	ReLU	512	MSE	378	0.10 m/s	72%	50%
		[8-515-886-346-1]	ReLU	128	MSE	209	0.10 m/s	71%	50%
	CDIR	[8-413-836-104-412-1]	ReLU	64	MAE	464	36.37^o	82%	54%
		[8-535-617-379-203-274-1]	ReLU	1024	MAE	197	36.47^o	81%	53%

Loading: Loading Condition of the Platform; **Target**: Variable estimated by the Neural Network; **Act.**: Activation Function; **Batch**: Batch size; **Loss**: Loss Function; **Pat.**: Patience Size; **R**: Pearson Correlation Coefficient; $\mathbf{R}^2$: Coefficient of determination; **MAE**: Mean Absolute Error

The attained results show that the *ReLU* activation function performs better than the other two functions (*Sigmoid* and *Tanh*). Besides that, when estimating current speed (*CVEL*), the Mean Square Error is the best choice as a cost function, while the Mean Absolute Error is the one for the current direction (*CDIR*).

With respect to the size of the Neural Networks, it can be noticed that estimating the current direction requires more complex architectures. This possibly demonstrates that it is harder to create models that capture hidden patterns between the input variables and the target one. Based on those results, the first MLP configuration for each target was chosen to perform estimation based on the test set.

3.2 Estimation of Ocean Currents

Figures 6 and 7 present the results for the full load condition. Those results refer to previously unseen data (test dataset). In the plots, the blue dots are the *MLP Estimations*, and the red ones denote the *Real data*.

For the current speed, one can infer that higher errors occur at higher and less common speeds (Figure 6a). Most of the time, the MLP underestimates the values. Despite that, in the majority of data, the estimations follow the references relatively well ($R = 70\%$ and $R^2 = 60\%$). This is expected once this algorithm is biased by the majority of moderate-speed data.

From the Error Distribution Analysis (Figure 6b), in the range of speeds $0.2 - 0.4 m/s$, almost 100% of the estimations are enclosed by 1-stdar deviation line. This indicates that in the most common speed range (from Figure 3), the estimations have an error of approximately 16% of the maximum error encountered.

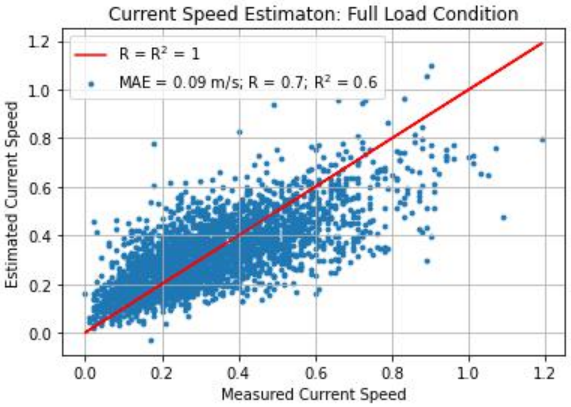

(a) Current Speed Estimation.

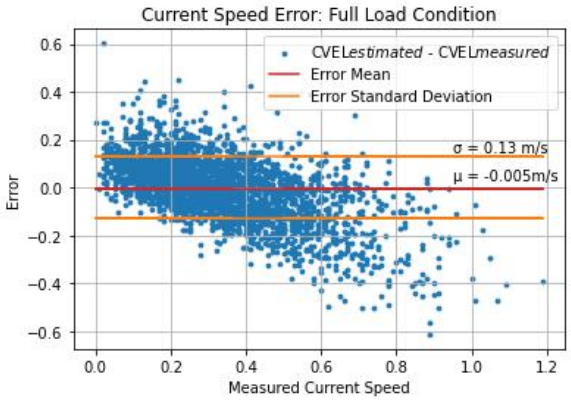

(b) Current Speed Error.

Figure 6: Current Speed $[m/s]$ Estimation: Full Load Condition

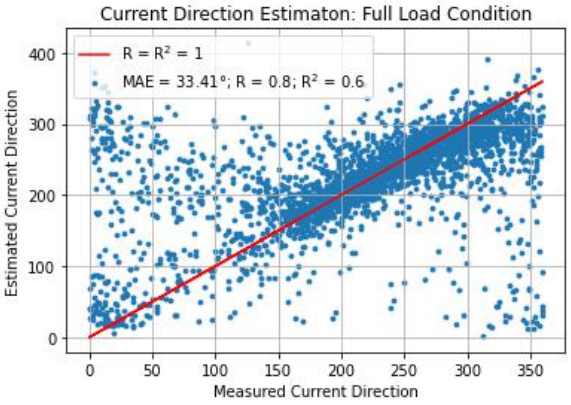

(a) Current Direction Estimation.

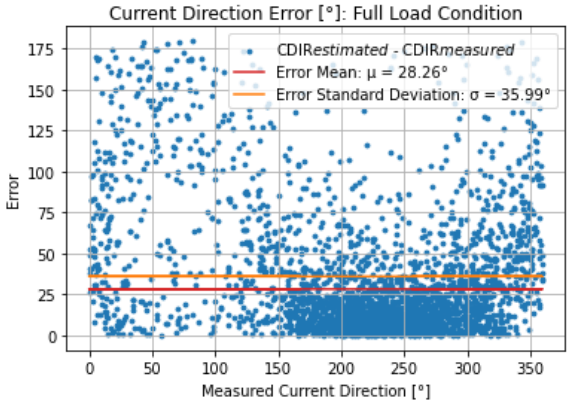

(b) Current Direction Error.

Figure 7: Current Speed Direction [^{o}] Estimation: Full Load Condition

Figures 7a and 7b give the estimations of the current direction. It is observed that in the range of directions $0^o - 150^o$, the estimations do not follow the target data, but these directions correspond to less than 20% of the data.

The results for the ballast condition (Figures 8 and 9) are similar to the ones for full load, but the metrics are relatively worse. This is also expected since the current influence on platform motion is draft-sensitive, and in this condition, the draft is 5 meters less.

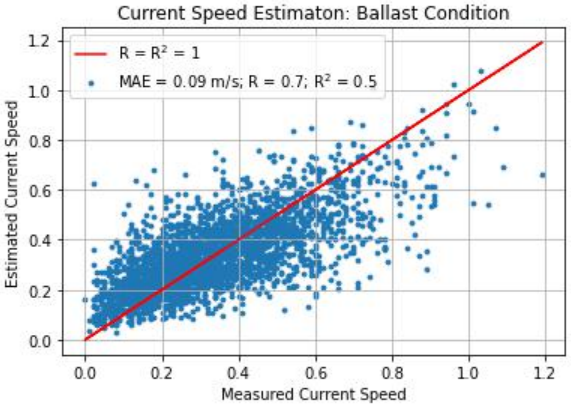

(a) Current Speed Estimation.

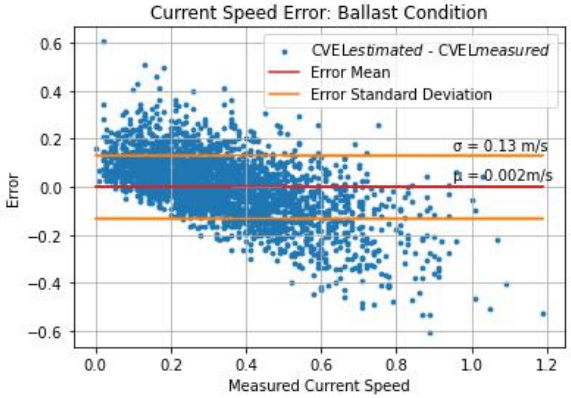

(b) Current Speed Error.

Figure 8: Current Speed $[m/s]$ Estimation: Ballast Condition

Similar conclusions concerning the intervals of higher errors are also valid here. About ocean current speed, Figure 8b indicates that the error mean value is positive ($\mu = 0.002m/s$), while for the full load (Figure 6b), it is negative ($\mu = -0.005m/s$). This implies that, for the ballast conditions, the Neural Networks correlate the more intense platform motions (Table 3) with higher values of current speed.

With respect to ocean current direction estimation, the mean value and standard deviation of the error (Figure 9b) is

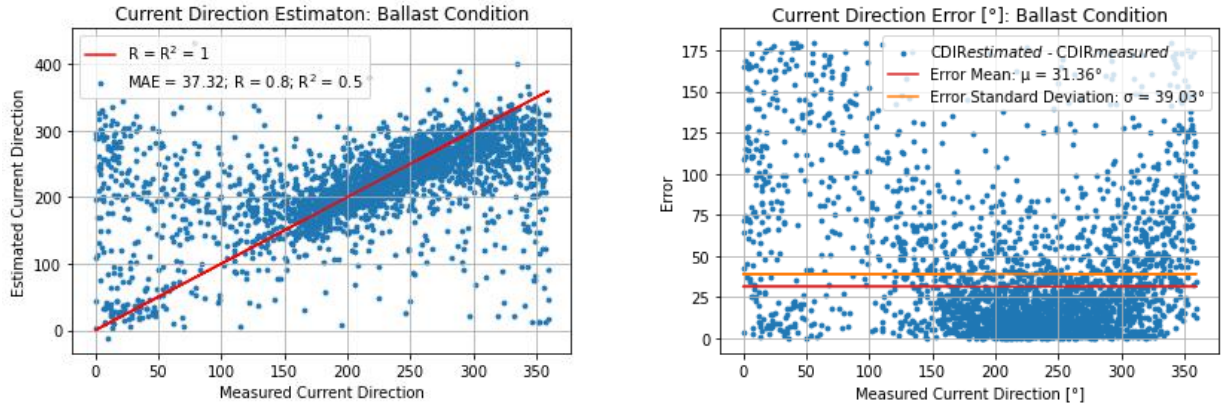

(a) Current Direction Estimation. (b) Current Direction Error.

Figure 9: Current Direction [^{o}] Estimation: Ballast Condition

more than 10% higher than for the full load condition (Figure 7b), and the same difficulties in the regions $N - NE - E - SE$ appear (Figure 9a).

Due to these issues, the post-processing strategy is proposed. It aims to capture some estimations that have less influence on platform motions and remove them from the dataset. It is expected most of this data to be located in the region of higher errors.

3.3 Post Processing Results

As previously explained, the post-processing method adds a domain-knowledge to the estimation results. Based on Eq. 6, the metric *Degree of Importance* is defined, which describes the ocean current potential effect on FPSO equilibrium heading.

Since the estimation of ocean current direction seems to be more challenging than speeds, the proposed technique aims to adjust only the results in the current direction. In practice, what is expected from the *Neural Estimator* is that: after estimating the current speed and direction, it computes the metric *Degree of Importance*, makes a *"yes/no type"* decision (based on the current direction estimation), and exhibits (or not) the estimated ocean current parameters to the user.

Figure 10 presents clusters of Current Direction Error per Degree of Importance. It is observed that the higher the errors (*y-axis*), the lower the relative relevancy of that current on the final heading. This finding is promising since it is expected that most of the estimations in the range of $0^o - 150^o$ can be discarded.

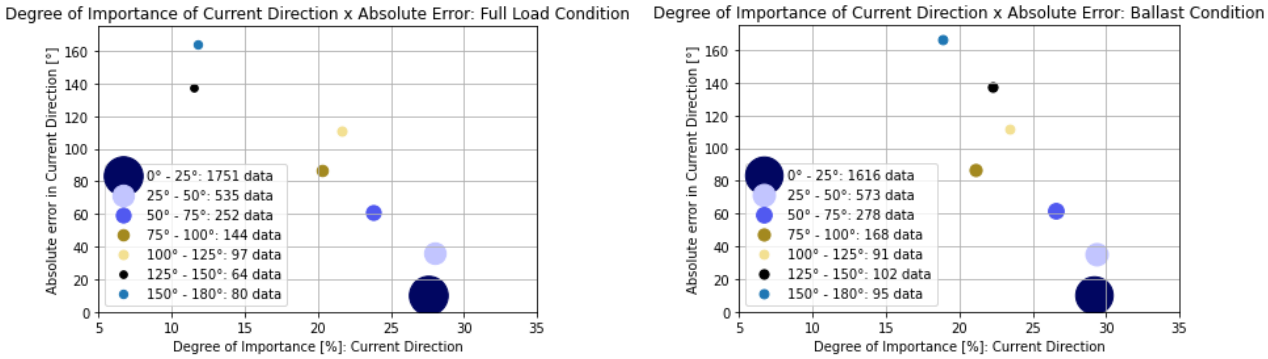

(a) Full Load Condition. (b) Ballast Condition.

Figure 10: Degree of Importance: Current Direction [^{o}]

Notice that each cluster in the previous figure represents the Mean of the Degree of Importance metric. This does not imply that all data in each cluster has the same *DoI*, but that the data in each cluster (based on absolute error) have the mean *DoI* presented in the *x-axis* of Figure 10. In this manner, the filtering at 30% will get rid of data in all seven clusters. After this filter, the test dataset was reduced by approximately 38% .

Figures 11a and 12a give the current direction estimation for full load and ballast conditions, respectively, after post-processing. From these figures, it is observed that the metrics have improved, supporting the assumption that the MLP errs more in the less common directions.

The error analysis shows that the Mean Absolute Error reduces almost 25% for the full load condition and 18% when in ballast. Also, the Standard Deviation of the Error is much closer to the Mean, indicating the lower variance of the estimations.

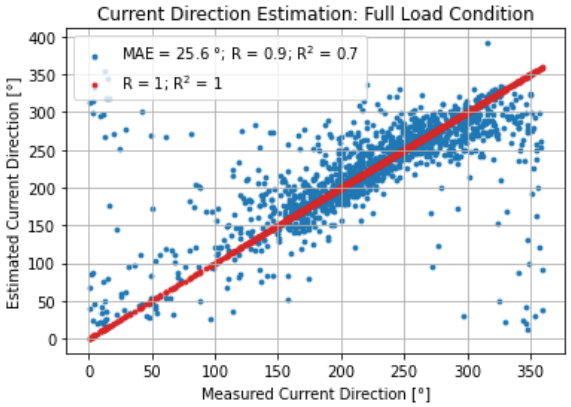

(a) Current Direction Estimation.

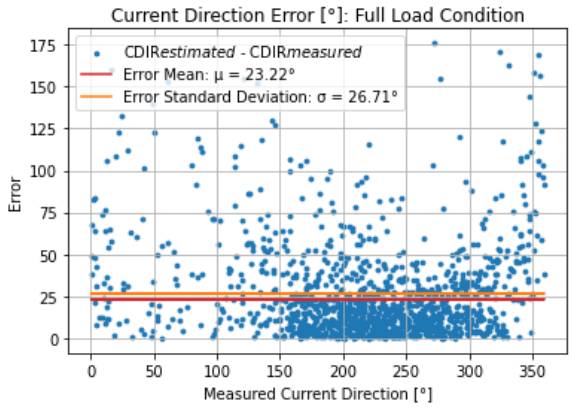

(b) Current Direction Error.

Figure 11: Estimation of Current Direction: Full Load Condition

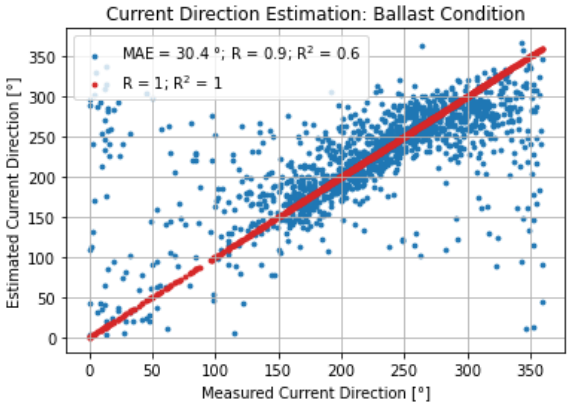

(a) Current Direction Estimation.

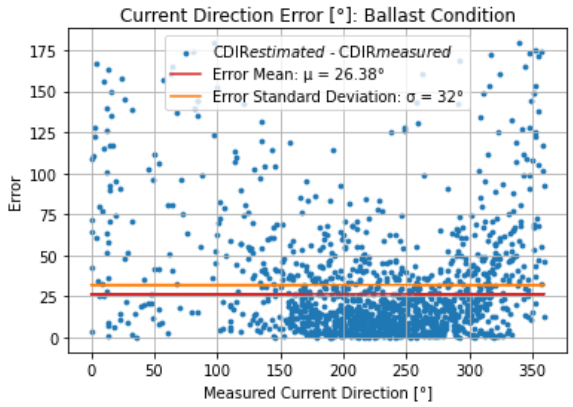

(b) Current Direction Error.

Figure 12: Estimation of Current Direction: Ballast Condition

In view of the above discussion, it is valid to affirm that the post-processing technique improved the estimations by adding information to the inverse problem, indicating that the proposed *Neural Estimator* is an initial good improvement for on-board estimation of ocean currents. Table 6 presents the Final Results, showing the Neural Architectures used and the metrics obtained after post-processing for each target estimated.

Table 6: Final Results

Loading	**Target**	**MLP configuration**					**Metrics**		
		Neurons per Layer	*Act.*	*Batch*	*Loss*	*Pat.*	*MAE*	*R*	R^2
Full Load	*CVEL*	[8-785-928-281-1]	ReLU	128	MSE	136	0.09 m/s	70%	60%
	CDIR	[8-746-201-332-157-668-1]	ReLU	512	MAE	342	25.6^o	90%	70%
Ballast	*CVEL*	[8-346-895-950-963-275-1]	ReLU	512	MSE	378	0.09 m/s	70%	50%
	CDIR	[8-413-836-104-412-1]	ReLU	64	MAE	464	30.4^o	90%	60%

Loading: Loading Condition of the Platform; **Target**: Variable estimated by the Neural Network; **Act.**: Activation Function; **Batch**: Batch size; **Loss**: Loss Function; **Pat.**: Patience Size; **R**: Pearson Correlation Coefficient; $\mathbf{R^2}$: Coefficient of determination; **MAE**: Mean Absolute Error

4. CONCLUSION

In this paper, Multi-Layer Perceptron Neural Networks were applied to estimate local ocean currents based on Turret-Moored FPSO movements. The motions consisted of: heading, standard deviation of heading (obtained by GPS or Magnetic/Gyro compass); and the standard deviation of heave, roll, and pitch (measured by MRU sensors). In addition to the motions, wind information (collected via anemometers/anemoscopes) is used as input to the *Neural Estimator*.

It was observed that, due to the directionality of the environmental conditions on the Brazilian coast, the dataset used to train the regressor algorithms is unbalanced, with a great amount of current data in the range of $0.2-0.4m/s$ speed that points to $SW-W-NW$ quadrants. This creates serious problems when dealing with data-driven applications. To reduce the hindrances originated by the dataset characteristic, a post-processing strategy was implemented which improved the results obtained.

A strong correlation between estimated and target variables (correlations of 70% and 90% for current speed and

direction, respectively, for the two loading conditions) was obtained. Together with a mean absolute error of 0.09 m/s and 25^o for full load condition, and 0.09 m/s and 30^o when in ballast. This demonstrates that the proposed method is a good approach for a hard, and yet, not common, task. Clearly, the identification of current properties was slightly more challenging as the draft was reduced.

To conclude, it is important to affirm that the platform motions are generated using simulated data, which bases its calculations on the equations of motions. This means that this research is still comparing results with numerical motion data. For future developments, the authors aim to implement the proposed algorithm with on-board measured motions.

5. ACKNOWLEDGEMENTS

This work was financed in part by the Coordenação de Aperfeiçoamento de Pessoal de Nível Superior (CAPES Finance Code 001), Brazil, and ANP/PETROBRAS, Brazil. We gratefully acknowledge partial support from CNPq (grants 310085/2020-9, and 310127/2020-3) and from São Paulo Research Foundation – FAPESP (process 2021/00409-2)

6. REFERENCES

Bisinotto, G.A., Sparano, J.V., Simos, A.N., Cozman, F.G., Ferreira, M.D. and Tannuri, E.A., 2023. "Sea state estimation based on the motion data of a moored fpso using neural networks: An evaluation with multiple draft conditions". *Ocean Engineering*, Vol. 276, p. 114235.

Brasil, A., 2020. "Anuario estatistico brasileiro do petroleo, gas natural e biocombustivel".

Dias, P.F.L., Bisinotto, G.A., Costa, A.H.R., Tannuri, E.A. and Caurin, G.A.d.P., 2022. "Estimation of ocean's currents acting on a turret-moored fpso using machine learning". *Proceedings of the ASME 2022 41st International Conference on Ocean, Offshore and Arctic Engineering*.

England, L., Duggal, A. and Allen, Q.L., 2001. "A comparison between turret and spread moored f(p)sos for deep water field developments". *Deep offshore technology*.

Faniband, Y.P. and Shaahid, S.M., 2020. "Forecasting wind speed using artificial neural networks – a case study of a potential location of saudi arabia". *ICACER*.

Goodfellow, I.; Bengio, Y. and Courville, A., 2016. *Deep Learning*. MIT Press.

Han, P., Li, G., Skjong, S., Wu, B. and Zhang, H., 2021. "Data-driven sea state estimation for vessels using multi-domain features from motion responses". *International Conference on Robotics and Automation*. doi: 0.1109/ICRA48506.2021.9561261.

Howell, G., Duggal, A. and Heyl, C. Ihonde, O., 2006. "Spread moored or turret moored fpso's for deep water field developments". *Offshore West Africa*.

Lima, J.A.M., Martins, R.P., Tanajura, C.A.S., Paiva, A.d.M., Cirano, M., Campos, E.J.D., Soares, I.D., Franca, G.B., Obini, R.d.S. and Avareng, J.B.R., 2013. "Design and implementation of the oceanographic modeling and observation network (remo) for operational oceanography and ocean forecasting". *Revista Brasileira de Geofisica*. ISSN 0102-261X.

Lobo, P.R.V., 2019. *Meteorologia e Oceanografia: Usuario ao Navegante*, Vol. I. Editora Vozes, 4th edition. ISBN 85-85966-13-0.

Nair, B.G., Vijayakumar, R. and Ananthakrishnan, P., 2019. "Hydrodynamic aspects of turret-moored fpsos". *Proceedings of the Fourth International Conference in Ocean Engineering (ICOE2018)*.

Nishimoto, K., Fucatu, C.H. and Masetti, I.Q., 2002. "Dynasim—a time domain simulator of anchored fpso". *OMAE2002*. ISSN 0892-7219. doi:10.1115/1.1513176. URL `https://doi.org/10.1115/1.1513176`.

Podrazka, O., Renac, L. and Enet, F., 2022. "On the calibration of metocean time series using machine learning". In *Proc. of the Int. Conf. on Offshore Mechanics and Arctic Engineering*.

Suller, T.M., Gomes, E.O., Oliveira, H.B., Cotrim, L.P., Sa'ad, A.M., Santos, I.H.F., Barreira, R.A., Costa, A.H.R. and Tannuri, E.A., 2021. "Evaluation of neural networks architecture search approaches for offshore platform offset prediction". *Brazilian Conference on Intelligent Systems*.

Tannuri, E.A., Fucatu, C.H., Massetti, I.Q., Rateiro, F., Ferreira, M.D. and Nishimoto, K., 2014. "Modular mathematical model for a low-speed maneuvering simulator". *Proceedings of the ASME 2014 33rd International Conference on Ocean, Offshore and Arctic Engineering*.

Thongniran, N., Jitkajornwanich, K., Lawawirojwong, S., Srestasathiern, P. and Vateekul, P., 2019. "Combining attentional cnn and gru networks for ocean current prediction based on hf radar observations". *Association for Computing Machinery*. doi:10.1145/3373509.3373549.

7. RESPONSIBILITY NOTICE

The authors are solely responsible for the printed material included in this paper.